

Supplemental Information

Pulse recruitment and recovery of Cayman Islands Nassau Grouper (*Epinephelus striatus*) spawning aggregations revealed by *in situ* length-frequency data

Brian C. Stock*, Scott A. Heppell, Lynn Waterhouse, India C. Dove, Christy V. Pattengill-Semmens, Croy M. McCoy, Phillippe G. Bush, Gina Ebanks-Petrie, and Brice X. Semmens

*brian.stock@noaa.gov

Quantity	M = 0.226 yr ⁻¹	M = 0.276 yr ⁻¹	M = 0.326 yr ⁻¹
2019 SSB/SSB ₀	0.87 (0.61, 1.23)	0.90 (0.65, 1.25)	0.92 (0.66, 1.27)
2009 SSB/SSB ₀	0.22 (0.16, 0.30)	0.23 (0.17, 0.32)	0.24 (0.18, 0.34)
2002 SSB/SSB ₀	0.40 (0.33, 0.48)	0.46 (0.39, 0.54)	0.52 (0.45, 0.59)
2011 Rec / mean Rec	6.5 (1.7, 11.3)	5.3 (0.6, 9.9)	4.5 (0.0, 9.1)
L _∞	80.2 (77.2, 83.3)	81.2 (78.1, 84.3)	82.2 (78.8, 85.5)
k	0.144 (0.128, 0.159)	0.141 (0.126, 0.156)	0.138 (0.123, 0.153)
a ₀	-0.79 (-0.94, -0.64)	-0.80 (-0.95, -0.65)	-0.82 (-0.97, -0.67)

Table S1. Sensitivity analysis of LIME-integrated model parameters and derived quantities to the assumed value of M. The results reported in main text used M = 0.276 yr⁻¹, and here we show results varying M by +/- 0.05 (18%). MLE are given with 95% CI in parentheses. Estimates of depletion (SSB / SSB₀) in the final year (2019) and minimum year (2009) are insensitive to specified M. Depletion in 2002, immediately following two years of heavy FSA fishing, is more sensitive to M and varies from 0.40 to 0.52. The 2011 recruitment spike is estimated for all values of M but varies in magnitude from 4.5 to 6.5x mean recruitment. The growth curve parameters are mildly sensitive to M.

Quantity	$h = 1, q = 1$	$h = 0.7$	$q = 0.9$	$q = 1.1$
2019 SSB/SSB ₀	0.90 (0.65, 1.25)	0.87 (0.62, 1.23)	0.94 (0.68, 1.31)	0.86 (0.62, 1.20)
2009 SSB/SSB ₀	0.23 (0.17, 0.32)	0.23 (0.17, 0.31)	0.25 (0.18, 0.34)	0.22 (0.16, 0.30)
2002 SSB/SSB ₀	0.46 (0.39, 0.54)	0.47 (0.40, 0.55)	0.47 (0.40, 0.56)	0.46 (0.39, 0.54)
2011 Rec / mean Rec	5.3 (0.6, 9.9)	5.6 (1.2, 9.9)	5.6 (0.9, 10.3)	5.1 (0.4, 9.7)
L_{∞}	81.2 (78.1, 84.3)	81.1 (77.9, 84.3)	81.1 (77.9, 84.4)	81.3 (78.1, 84.4)
k	0.141 (0.126, 0.156)	0.142 (0.126, 0.157)	0.141 (0.125, 0.157)	0.141 (0.126, 0.156)
a_0	-0.80 (-0.95, -0.65)	-0.80 (-0.95, -0.65)	-0.81 (-0.96, -0.65)	-0.80 (-0.95, -0.65)

Table S2. Sensitivity analysis of LIME-integrated model parameters and derived quantities to the assumed value of steepness, h , and survey catchability, q . The results reported in main text used $h = 1$ and $q = 1$ (left column), and here we show results using $h = 0.7$, $q = 0.9$, and $q = 1.1$. MLE are given with 95% CI in parentheses. Most estimates are nearly identical, with the most difference in depletion (SSB / SSB₀) in the final year and the 2011 recruitment spike.

Laser caliper calibration, measurement error, and data collection

We calibrated the new laser caliper systems before each dive to be within 19.5–20.5 cm at 10 m. On a given dive, the operator turned on the video camera and lasers, and placed the laser points on a dive slate held perpendicularly to the laser axis by their dive buddy, while the dive buddy swam away until the laser points could not be seen. The operator then moved to the far end of the aggregation and swam slowly back to the starting point, placing the laser points on fish that were perpendicular to the camera for ~3 s per fish. The first step to obtain length measurements from the video is to capture still frames where the laser points are on a fish, capturing a frame where the fish is as close to perpendicular to the camera as possible, and fully in view, and the fish is straight (tail not curved). We then opened the still frames in ImageJ software, used the measurement of the laser points on the dive slate to set the scale (pixels cm⁻¹), and measured the total length of the fish.

We estimated the measurement error of the laser caliper method by a similar analysis to Heppell et al. (2012). For two objects of known size (55.72 and 60.96 cm), we replicated the above method at 2 and 4 m, and increasing angles offset from perpendicular (0°, 5°, 10°, 15°, 20°, 25°, and 30°). For both distances, the measurement error was 5–7% at angles less than 10° (Fig. S1). Beyond 10°, measurement error increased to 10–20%. Although we did not do a formal test to determine at which angles video analysts rejected images, analysts felt they would begin to reject images at angles > 10°. These results, including analyst rejection of off-axis images, is similar to that observed by Heppell et al (2012).

Nassau Grouper at the Little Cayman FSA typically spawn in either January or February, depending on when the full moon falls in the month; if the full moon is in late January and late February, major spawning is likely to be in January, and vice-versa if full moon occurs early in those months). When full moons fall in the middle of the month, it is difficult to know whether major spawning will be in January or February. Thus, in some years we collected length data from both major and minor spawning months. We found no differences in length distributions between major and minor spawning months across years, and therefore pooled all data within years in subsequent analyses (Fig. S2). No differences in length have been found by any of the other auxiliary variables we record: location (resting on bottom vs. up in water column), color phase, time of day, or day before peak spawning.

In 2018 we used an alternative method, a stereo camera system (described in Williams et al. 2010), to collect *in situ* length measurements from the east end Cayman Brac FSA. In contrast to the laser calipers, which can only measure one fish at a time and must be diver-operated, stereo systems effectively build a 3-dimensional image from two synchronized cameras and can measure objects anywhere in their field of view. Thus, they can be used remotely (either baited or un-baited; Watson et al. 2005) and may be more efficient for monitoring FSA size structure. To confirm that the stereo camera produced comparable length measurements, we attached the laser calipers to the stereo camera for two dives and measured all fish with laser points in the stereo camera images. We found good agreement between the length measurements produced by the two systems (Fig. S3). Since they reconstruct 3-dimensional coordinates, stereo cameras also can estimate the distance to objects in images. These estimates confirmed that most of our distances-to-fish when using the laser calipers were between 3–4 m, and all were between 2–5 m.

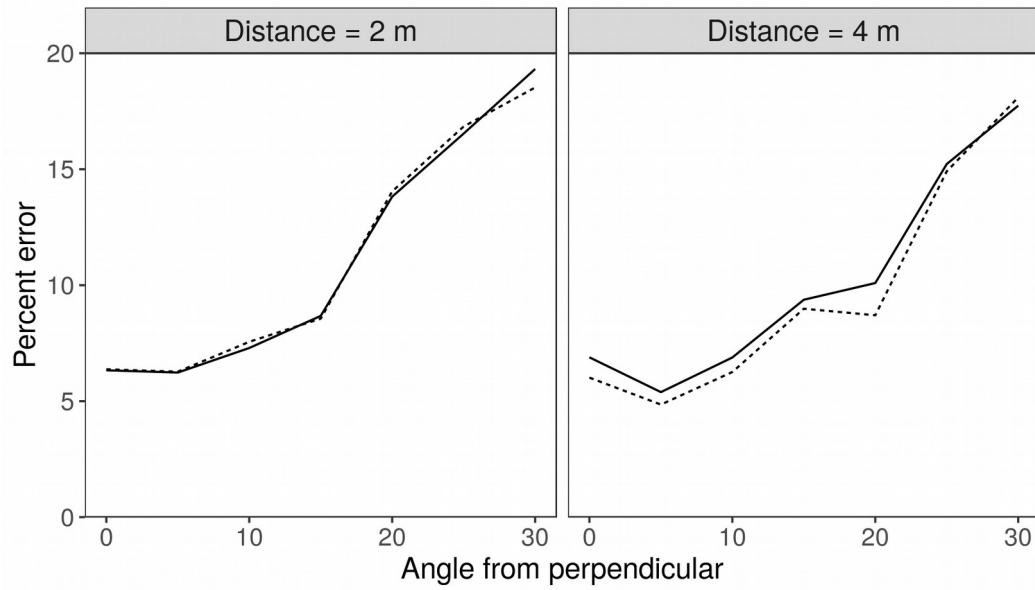


Figure S1. Measurement error of the laser caliper system as a function of distance-to-camera and angle offset from perpendicular. Two objects of known size typical of Nassau Grouper (55.72 and 60.96 cm, line type) were measured at 2 and 4 m distance and 0–30° from perpendicular. Measurement error was 5–7% at angles less than 10° and increased rapidly beyond 15°.

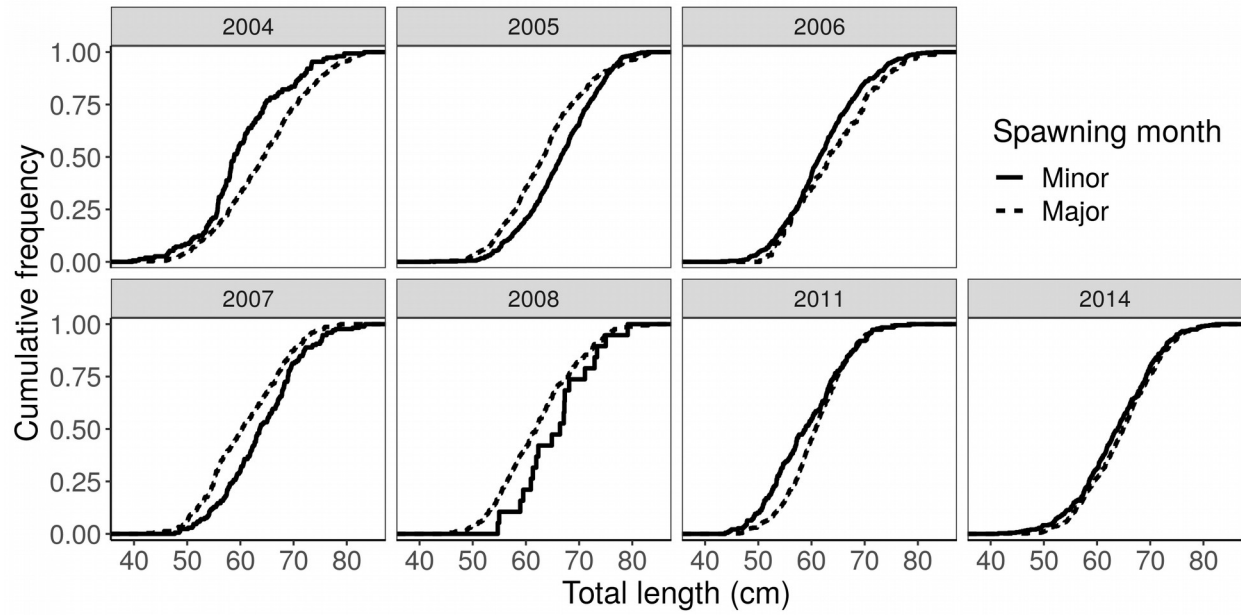


Figure S2. Length distributions for major versus minor spawning months. Fish lengths in major spawning months were larger in 4 out of 7 years (dashed curve right of solid curve; 2004, 2006, 2011, 2014), and smaller in the other 3 years (dashed curve left of solid curve; 2005, 2007, 2008).

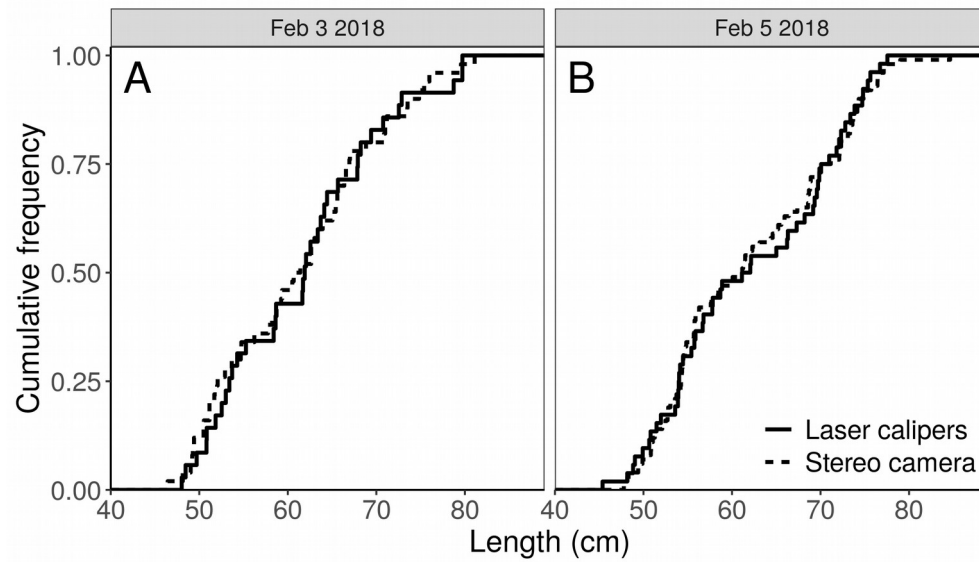


Figure S3. Length distributions measured from the stereo camera (dashed line) and laser calipers (solid line). On two dives the laser calipers were attached to the stereo camera and all fish with laser points in the stereo camera images were measured using both systems.

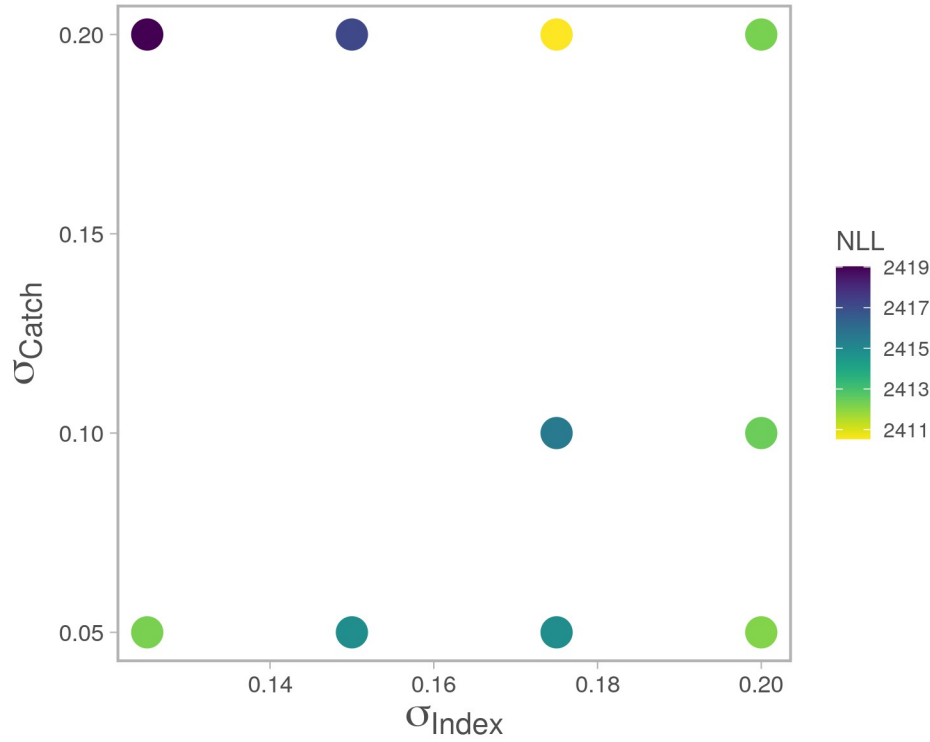


Figure S4. Sensitivity analysis of the LIME-integrated model to data weighting parameters σ_c (catch observation error: 0.05, 0.1, and 0.2) and σ_i (abundance index observation error: 0.1, 0.125, 0.15, 0.175, and 0.2). The negative log-likelihood was optimized at $\sigma_c = 0.20$ and $\sigma_i = 0.175$ (yellow point), and these values were used in the final LIME-integrated model (Fig. 8). We did not consider values of above 0.2 for σ_c because we have high confidence in the estimates of catch from the Little Cayman FSA in 2001 and 2002.

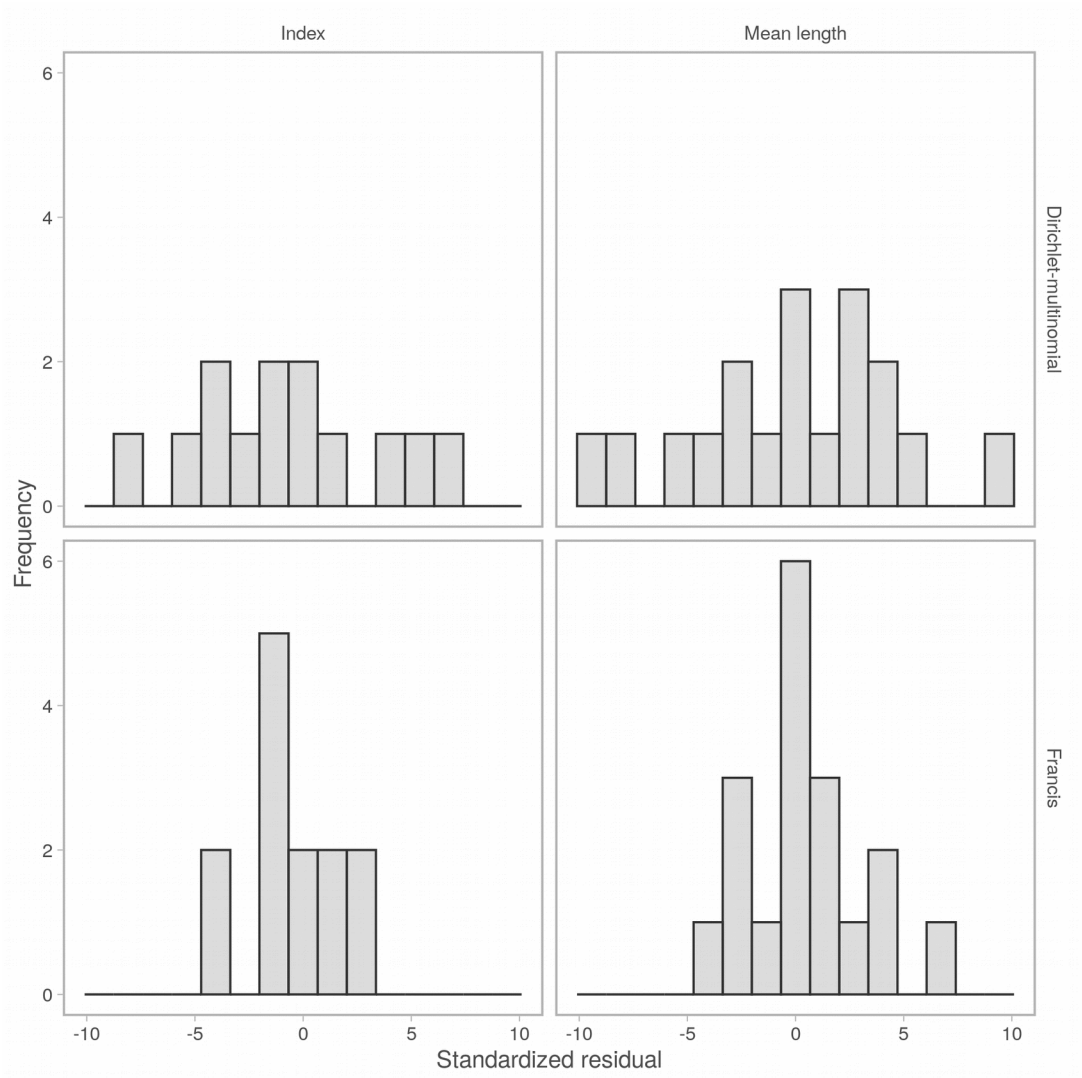


Figure S5. Distributions of standardized residuals for the index and mean length from the LIME-integrated model with Dirichlet-multinomial (top row) versus Francis weighting (bottom row).

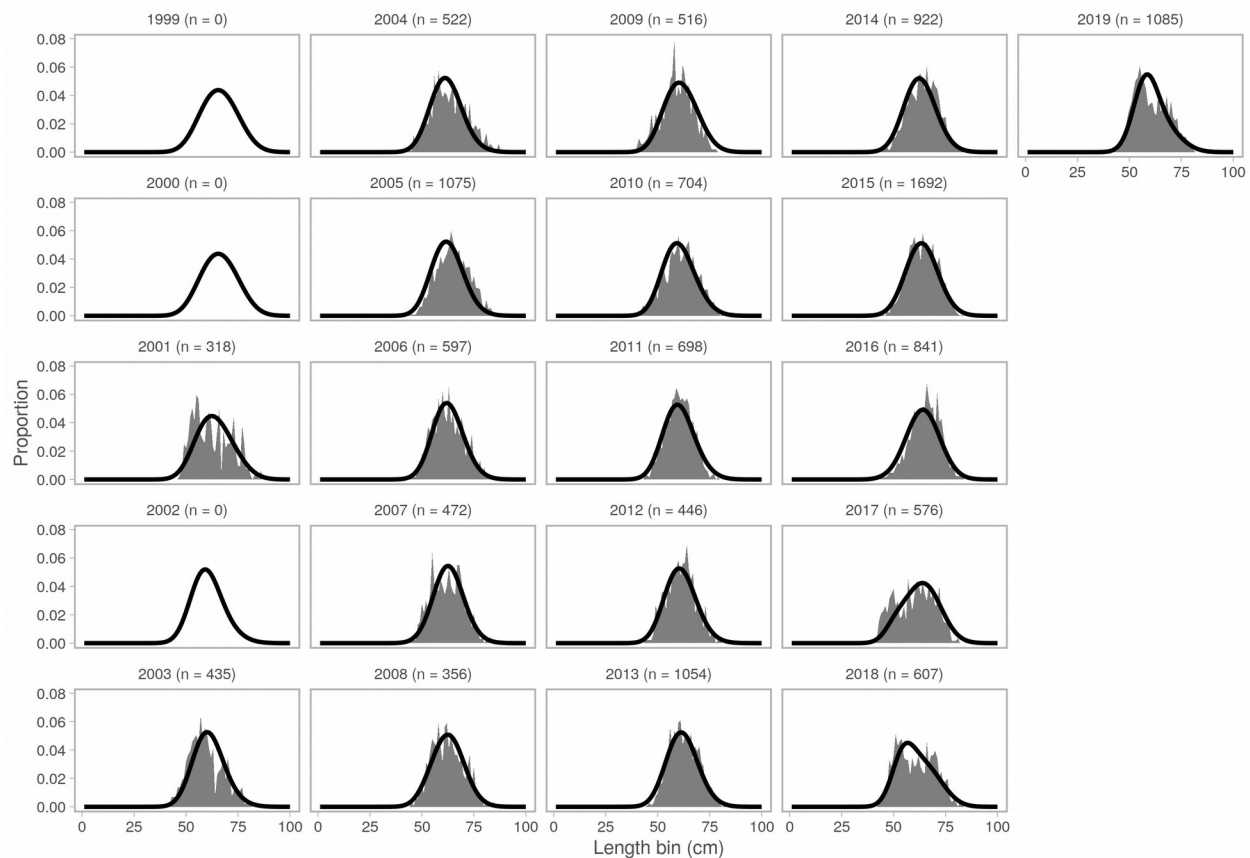


Figure S6. Fits to the Little Cayman FSA length-frequency data from the LIME-integrated model with Francis weighting. Histograms show raw length data and curves show model fits.

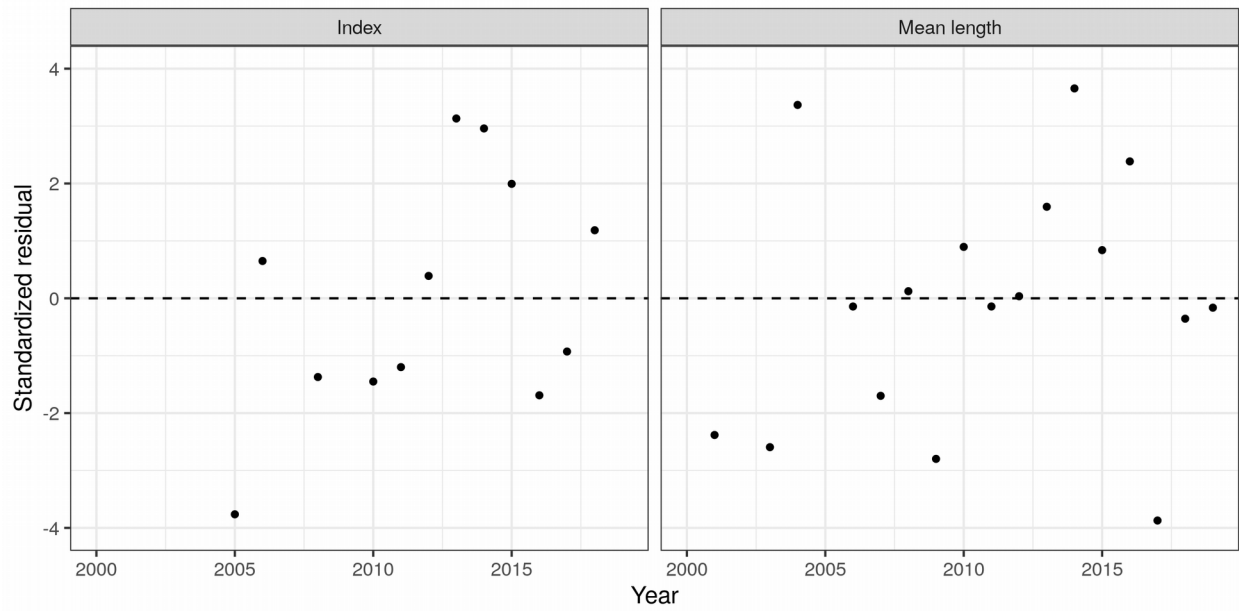


Figure S7. Standardized residuals for the index and mean length from the LIME-integrated model with Francis weighting. The residual for mean length in 2005 was > 4 (off chart).

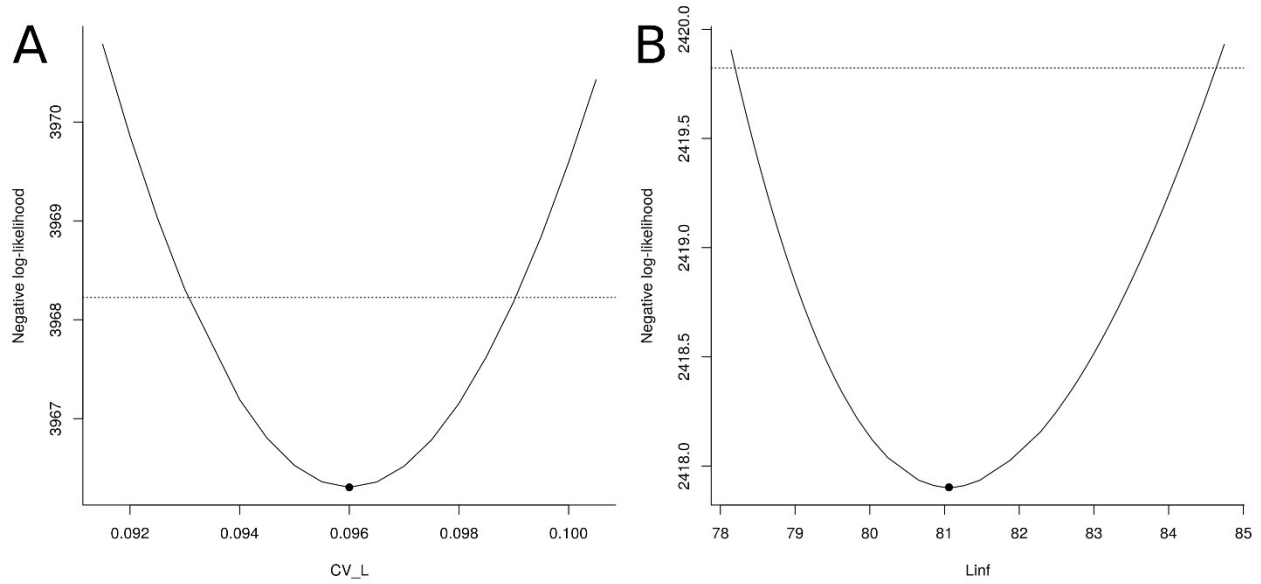


Figure S8. Likelihood profiles for A) the coefficient of variation of length-at-age, CV_L , and B) von Bertalanffy asymptotic length, L_{∞} . In A), models that estimated CV_L failed to converge. However, a grid search with CV_L ranging from 0.08-0.11 found that the negative log-likelihood was minimized at $CV_L = 0.096$ (black point), and this value was used in the final LIME-integrated model (Fig. 8).

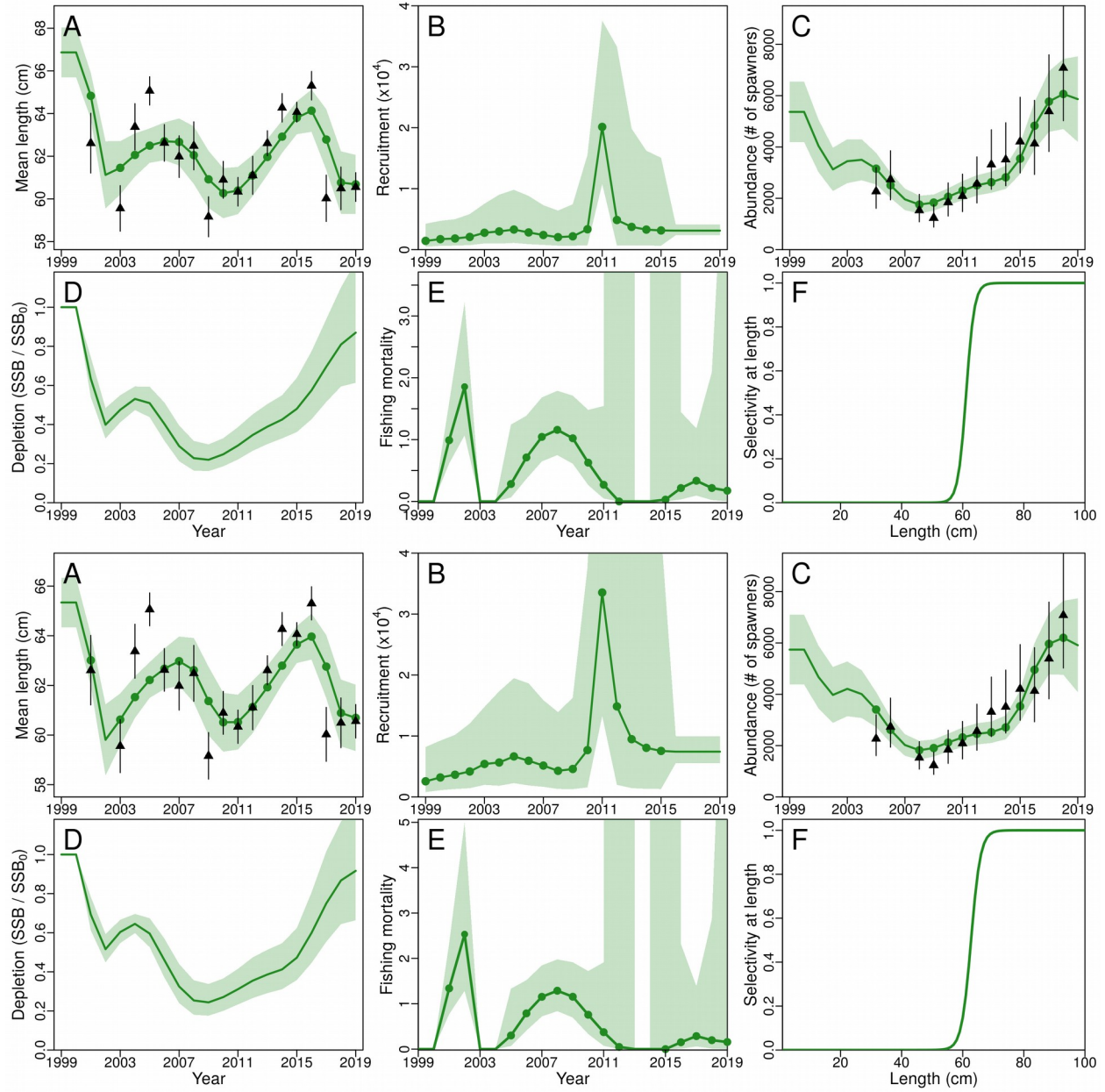


Figure S9. Sensitivity analysis of the LIME-integrated model to assumed value of M . The results reported in main text used $M = 0.276 \text{ yr}^{-1}$, and here we show results varying M by ± 0.05 (18%). Upper panels: $M = 0.226 \text{ yr}^{-1}$. Lower panels: $M = 0.326 \text{ yr}^{-1}$.

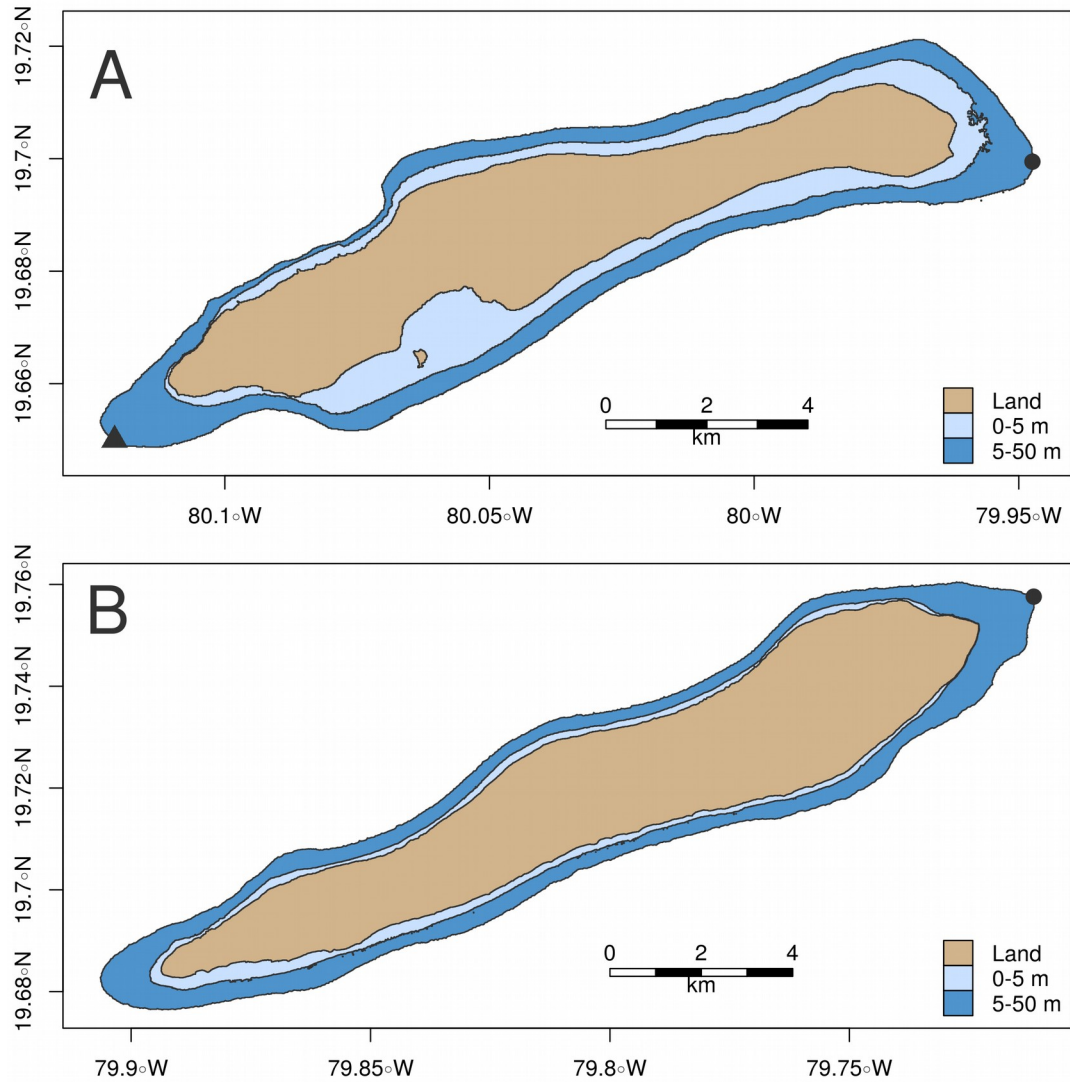


Figure S10. Habitat area available to Nassau Grouper on Little Cayman and Cayman Brac. A) Little Cayman has 1,440 ha of adult habitat area (5–50 m depth, dark blue) and 1,315 ha of juvenile habitat area (0–5 m depth, light blue). B) Cayman Brac has 1,689 ha of adult habitat and 572 ha of juvenile habitat. FSA locations are depicted by black points at the west (current) and east (historic) ends of Little Cayman, the east end of Cayman Brac. We calculated adult habitat area using high-resolution bathymetry (R packages ‘raster’ v2.8-4 and ‘sf’ v0.7-1; Hijmans 2018; Pebesma 2018).

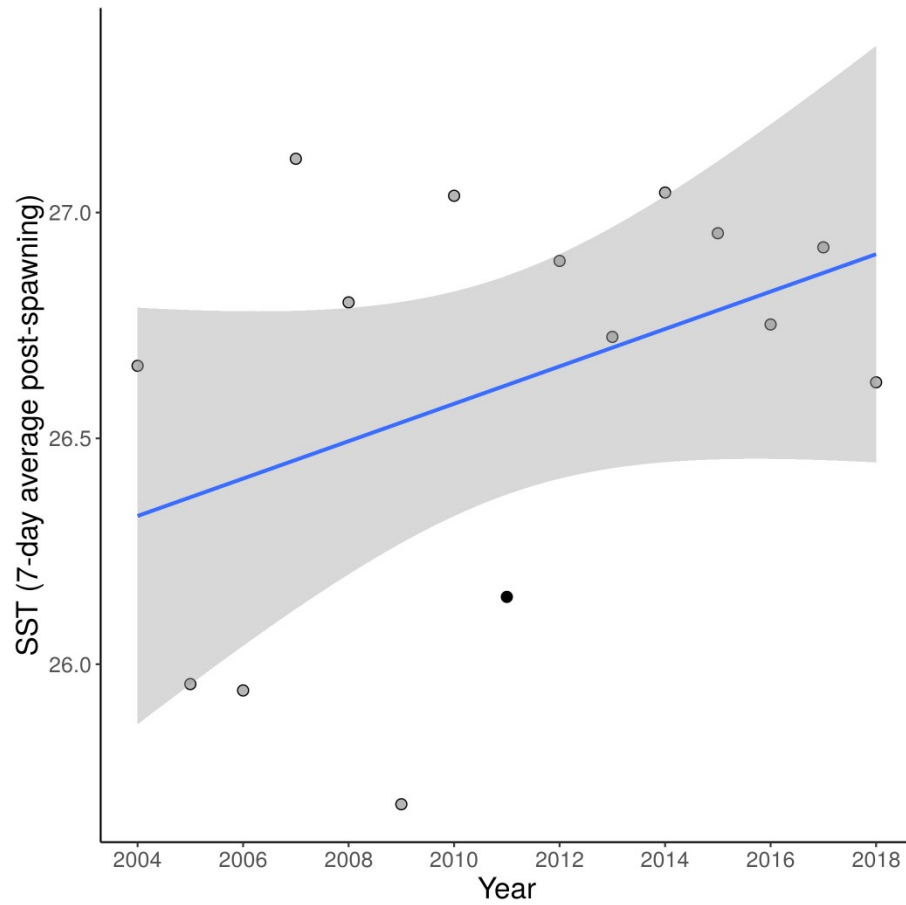


Figure S11. Sea surface temperature surrounding Little Cayman after spawning events from 2004–2018, 7-day average. The black point distinguishes 2011, the year with the (age-0) recruitment spike. For each year, peak spawning dates were recorded by divers from CIDOE and REEF. Temperature was averaged for the 7 days following each spawning date over latitude 19.6–19.8 °N and longitude 80.15–79.70 °W. Temperature data were downloaded from <https://podaac.jpl.nasa.gov/dataset/MUR-JPL-L4-GLOB-v4.1>.